

Statistical–Dynamical Seasonal Forecast for Tropical Cyclones Affecting New York State

HYE-MI KIM, EDMUND K. M. CHANG, AND MINGHUA ZHANG

School of Marine and Atmospheric Sciences, Stony Brook University, Stony Brook, New York

(Manuscript received 6 August 2014, in final form 15 December 2014)

ABSTRACT

This study attempts, for the first time, to predict the annual number of tropical cyclones (TCs) affecting New York State (NYS), as part of the effort of the New York State Resiliency Institute for Storms and Emergencies (RISE). A pure statistical prediction model and a statistical–dynamical hybrid prediction model have been developed based on the understanding of the physical mechanism between NYS TCs and associated large-scale climate variability. During the cold phase of El Niño–Southern Oscillation, significant circulation anomalies in the Atlantic Ocean provide favorable conditions for more recurving TCs into NYS. The pure statistical prediction model uses the sea surface temperature (SST) over the equatorial Pacific Ocean from the previous months. Cross validation shows that the correlation between the observed and predicted numbers of NYS TCs is 0.56 for the June 1979–2013 forecasts. Forecasts of the probability of one or more TCs impacting NYS have a Brier skill score of 0.35 compared to climatology. The statistical–dynamical hybrid prediction model uses Climate Forecast System, version 2, SST predictions, which are statistically downscaled to forecast the number of NYS TCs based on a stepwise regression model. Results indicate that the initial seasonal prediction for NYS TCs can be issued in February using the hybrid model, with an update in June using the pure statistical prediction model. Based on the statistical model, for 2014, the predicted number of TCs passing through NYS is 0.33 and the probability of one or more tropical cyclones crossing NYS is 30%, which are both below average and in agreement with the actual activity (0 NYS TCs).

1. Introduction

Landfalling tropical cyclones (TCs) represent one of the most destructive kinds of weather systems. These storms bring about high winds, heavy rain, and storm surge that can lead to substantial losses in life and property. Recent storms, such as Sandy in 2012 and Irene in 2011, have provided reminders that the heavily populated northeastern United States is an area that is prone to being affected by TCs. Given their significant impacts, accurate seasonal forecasts of TC activity might allow emergency management to become better prepared to help mitigate their effects. One of the missions of the New York State (NYS) Resiliency Institute for Storms and Emergencies (RISE)—a consortium of Stony Brook University, New York University, Columbia University, Cornell University, City University of New York, and

Brookhaven National Laboratory—is to help prepare stakeholders for extreme weather events. To that end, an assessment has been made to evaluate existing seasonal predictions of TC activity that impacts New York State.

The Climate Prediction Center (CPC) of the National Oceanic and Atmospheric Administration (NOAA), in collaboration with the National Hurricane Center (NHC) and the Hurricane Research Division (NRD), issues an Atlantic hurricane season outlook every May, with an update issued in August. However, the outlook is for TC activity that affects the entire Atlantic basin, and no regional predictions are made. Recently, the Tropical Meteorology Project of Colorado State University started issuing seasonal hurricane landfall probabilities for states and counties along the Gulf and Atlantic coasts (<http://www.e-transit.org/hurricane/welcome.html>). The current-year seasonal predictions of regional probabilities are based on scaling the climatological hurricane landfall probabilities by seasonal predictions of basinwide net TC activity. While this strategy may work for many locations, forecasts based on rescaling basinwide predictions are not

Corresponding author address: Edmund K. M. Chang, 101 Endeavour Hall, School of Marine and Atmospheric Sciences, Stony Brook University, Stony Brook, NY 11794-5000.
E-mail: kar.chang@stonybrook.edu

expected to work well for New York State. As will be discussed in [section 2](#), only a small percentage of Atlantic basinwide TCs affect New York State, and the correlation between basinwide TCs and those affecting New York State is low, thus even a perfect basinwide forecast is of limited value for New York State. Therefore, to advance the seasonal prediction of TCs affecting New York State, a new seasonal prediction model is required by revisiting the associated physical mechanisms.

Numerous studies have shown that Atlantic TC activity is highly influenced by large-scale circulation anomalies, particularly those related to sea surface temperature anomalies (SSTAs) over the Pacific characterized by El Niño–Southern Oscillation (ENSO). The cold phase of ENSO is associated with enhanced TC activity in both basinwide and landfalling storms through changes in atmospheric steering, vertical wind shear (VWS), and thermodynamic conditions ([Gray 1984](#); [Goldenberg and Shapiro 1996](#); [Bove et al. 1998](#); [Elsner 2003](#); [Tang and Neelin 2004](#); [Camargo et al. 2007b](#); [Smith et al. 2007](#); [Kossin et al. 2010](#); among many others). ENSO has been known to have a greater impact on recurving landfalling TCs than other climate modes, while the North Atlantic Oscillation (NAO) and Atlantic meridional mode (AMM) also have a significant impact on landfalling TCs ([Elsner 2003](#); [Vimont and Kossin 2007](#); [Kossin et al. 2010](#); [Klotzbach 2011](#); [Colbert and Soden 2012](#); among many others). In particular, the U.S. East Coast experiences the most dramatic differences between ENSO phases where the percentage of recurving landfall TCs that affect the U.S. East Coast increases during La Niña because of the change in the large-scale steering flow over the mid-Atlantic ([Smith et al. 2007](#); [Klotzbach 2011](#); [Colbert and Soden 2012](#)).

While many previous studies examined the impact of ENSO on landfalling TCs, only a few studies focused on the impact on U.S. subregions. [Klotzbach \(2011\)](#) found that the probability of North Carolina being impacted by a hurricane is strongly modulated by ENSO phases, while no significant change is detected in New York State and New Jersey. [Klotzbach \(2011\)](#) focused on the hurricane category over the period of 1900–2009, which includes the inhomogeneous storm data during the presatellite era. However, many storms that caused high impact weather over New York State were not hurricanes, but tropical storms, tropical depressions, or extratropical cyclones when the TCs crossed NYS, hereafter referred to as NYS TCs. Therefore, the relationship between large-scale climate variability and TCs affecting NYS needs to be revisited with more accurate storm datasets and with all storms included regardless of the stage of their life cycle. Improved understanding of the physical mechanism responsible for the TCs crossing NYS would also improve our capability of predicting them.

Seasonal TC prediction models have been classified as either a pure statistical model or a dynamical model [overview in [Camargo et al. \(2007a\)](#)]. However, recent studies have shown an improvement in seasonal TC prediction by combining the statistical and dynamical approaches ([Wang et al. 2009](#); [Kim and Webster 2010](#); [Vecchi et al. 2011](#); [Kim et al. 2013](#); [Li et al. 2013](#)). In this study, we develop an advanced statistical–dynamical hybrid model to improve seasonal prediction for NYS TCs based on the physical understanding of the relationship with large-scale ocean–atmosphere circulation. [Section 2](#) describes the data. The relationship between seasonal NYS TC activity and large-scale climate variability is examined in [section 3](#). Models for seasonal NYS TC prediction are introduced and verified in [section 4](#). Results are summarized and discussed in [section 5](#).

2. Data

a. Storm data

Best-track data for Atlantic TCs from the Hurricane Data 2nd generation (HURDAT2; [Landsea and Franklin 2013](#)) have been analyzed for the years 1979–2013. All TCs passing through NYS during any time of their life cycle have been identified. A total of 18 storms in 15 seasons passed over NYS during these 35 years. The tracks of these storms have been plotted in [Fig. 1a](#). The years of occurrence, names, and categories of these TCs are listed in [Table 1](#). During these years, only one hurricane (Gloria in 1985) made landfall over NYS. Seven storms were tropical storms when they crossed NYS, three were tropical depressions, and the remaining were extratropical events.

Impacts of the 18 storms ([Table 1](#)) on NYS have been assessed using the CPC daily (1200–1200 UTC) gridded continental U.S. precipitation analysis ([Higgins et al. 1996](#)), and 3-hourly surface wind analysis from the North American Regional Reanalysis (NARR; [Mesinger et al. 2006](#)). Most of these storms, including storms other than hurricanes, had very significant impacts over NYS. For example, Irene in 2011 was downgraded to a tropical storm just before landfall, but the storm surge of 3–6 ft caused hundreds of millions of dollars in property damage in New York City and Long Island ([Avila and Cangialos 2011](#)). Floyd in 1999 was a tropical storm when it passed over NYS, but it provided the heaviest 24-h precipitation (more than 8 in.) over NYS during 1979–2013, as well as surface winds of over 20 m s^{-1} (within the top 0.05% during the same period). Andrea, Frances, and Opal were extratropical storms when they crossed NYS, but all produced over 4 in. of rainfall in a day (within the top 0.5% of all days over the period).

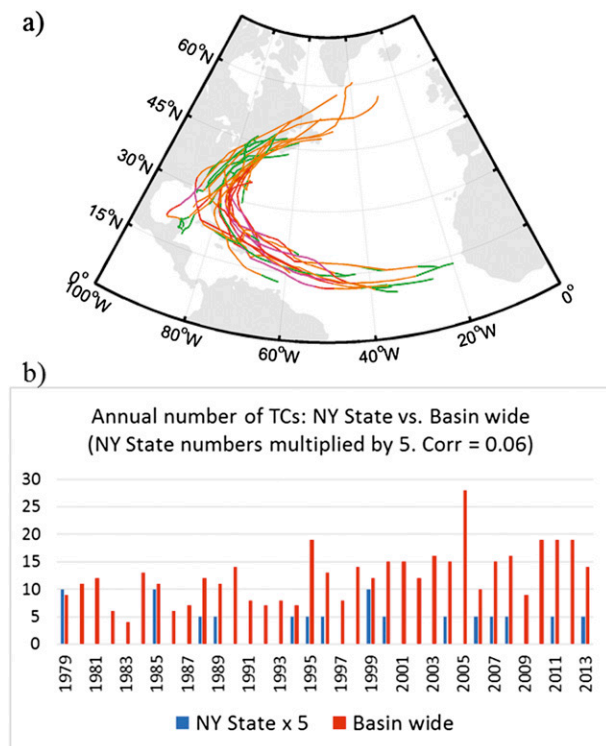


FIG. 1. (a) Tracks of all TCs that passed through NYS during 1979–2013. The color code relates to wind speed: green, ≤ 33 knots (kt ; $1 \text{ kt} = 0.51 \text{ m s}^{-1}$); orange, 34–63 kt ; red, 64–95 kt ; and purple, $\geq 96 \text{ kt}$. (b) Number of TCs passing through NYS (blue bars, numbers multiplied by 5) vs basinwide number of TCs (red bars) for each year.

Other storms such as Ernesto in 2006, which again was extratropical when crossing NYS, gave rise to very strong winds (17.9 m s^{-1} ; within the top 0.5% during 1979–2013) over eastern Long Island. Overall, 11 of the 18 storms gave rise to precipitation or winds (or both) that ranks within the top 1%. Of the remaining seven, three storms had impacts that are within the top 2%, and two were within the top 5%. Only two storms (Dennis and Henri) did not give rise to significant impacts over NYS. Since most of these storms caused high impact weather over NYS, we decided to analyze statistics of all storms that crossed NYS regardless of the stage of their life cycle when they crossed the state.

The number of storms crossing NYS each year is plotted in Fig. 1b, together with the total number of storms over the Atlantic basin. It can be seen that between zero and two storms crossed NYS each year. It is also apparent that the number of storms crossing NYS and the total number of storms over the Atlantic basin are not closely related. In fact, the correlation between these two numbers is only 0.06 over these 35 years. In addition, the correlation between the basinwide Accumulated Cyclone Energy (ACE; Bell et al. 2000) and the

TABLE 1. Year, name, and category of TCs crossing NYS between 1979 and 2013.

Year	Name	Category when crossing NYS
1979	David	Tropical storm
	Frederic	Tropical storm
1985	Gloria	Hurricane
	Henri	Tropical storm
1988	Chris	Tropical depression
1989	Hugo	Extratropical
1994	Beryl	Tropical depression
1995	Opal	Extratropical
1996	Bertha	Tropical storm
1999	Dennis	Tropical depression
	Floyd	Tropical storm
2000	Gordon	Extratropical
2004	Frances	Extratropical
2006	Ernesto	Extratropical
2007	Barry	Extratropical
2008	Hanna	Tropical storm
2011	Irene	Tropical storm
2013	Andrea	Extratropical

number of storms crossing NYS is 0.20. Hence, as discussed in section 1, even perfect seasonal forecasts of the basinwide tropical cyclone statistics will not be particularly useful for predicting the number of storms crossing NYS.

b. Observation and reforecasts

For statistical–dynamical hybrid prediction, seasonal reforecasts from NCEP Climate Forecast System, version 2 (CFSv2; Saha et al. 2014), have been used as the predictor field. CFSv2 became operational in 2011, and has shown significant improvements in its prediction skill compared to the previous version. For CFS reforecasts, initial conditions for the atmosphere and ocean come from the NCEP CFS Reanalysis (CFSR; Saha et al. 2010). CFSR is the product of a coupled ocean–atmosphere–land system and the resolution of the spectral atmospheric model is T382 ($\sim 40 \text{ km}$) with 64 vertical levels.

CFSv2 reforecasts are a set of 9-month reforecasts initiated every fifth day with four ensemble members each day for the period from 1982 to 2009. For example, for our forecast issued in the month of February, CFSv2 predictions from initial conditions at 0000, 0600, 1200, and 1800 UTC on 11, 16, 21, 26, and 31 January, and 5 February (<http://cfs.ncep.noaa.gov/>) are used. This results in an ensemble size of 24 CFSv2 forecasts that are used in our hybrid statistical–dynamical forecast issued near the beginning of each month. In this analysis, forecast month indicates the month when the forecast is issued. Previous studies suggest that there are significant differences in the SST climatology before and after 1999 in the CFSv2 hindcasts (Barnston and Tippett 2013; Xue et al. 2013). Therefore, anomalies are calculated

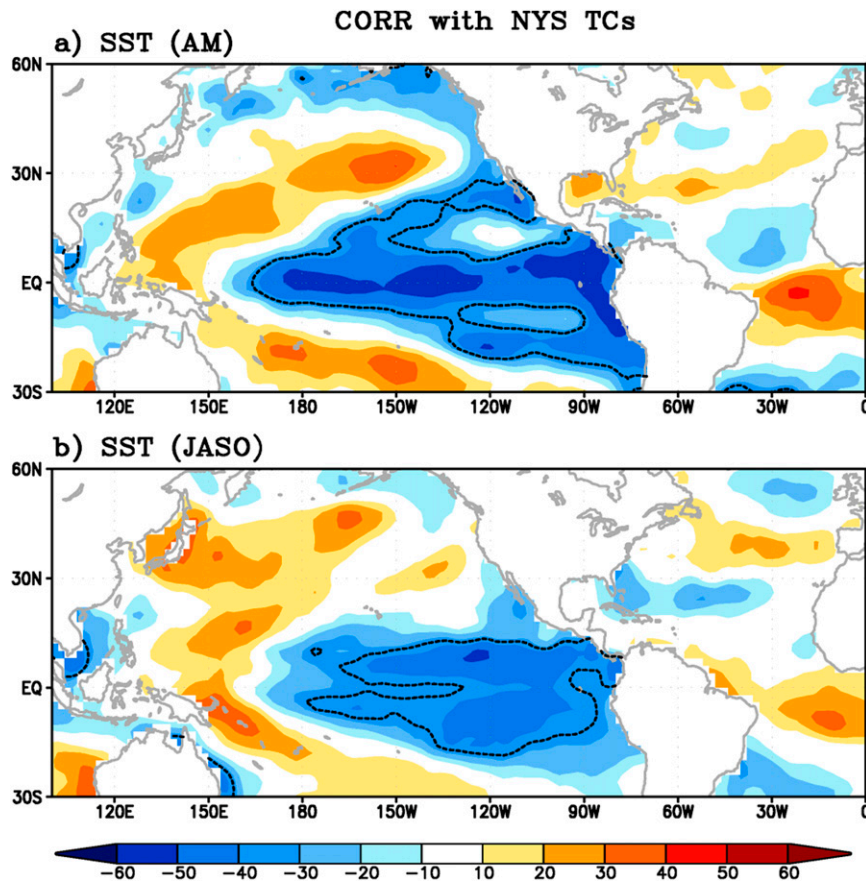


FIG. 2. The spatial distribution of correlation coefficients ($\times 100$) between the number of NYS TCs and SSTA averaged over (a) AM and (b) JASO. The black lines denote the negative threshold values for the 90% confidence level based on the FDR test.

based on the climatology for 1982–98 and 1999–2009 separately.

Observed monthly SST data are obtained from the NOAA Extended Reconstructed SST, version 3b (ERSST.v3b; [Smith et al. 2008](#)), dataset. Zonal wind, mean sea level pressure (MSLP), and geopotential height (GPH) data at various vertical levels are obtained from ERA-Interim ([Berrisford et al. 2009](#)). The vertical wind shear (VWS) magnitude is defined as the magnitude of the difference in the zonal wind between 850 and 200 hPa. The anomalies are obtained from a 35-yr climatology (1979–2013).

3. Physical basis for seasonal NYS TC forecast

A physical understanding of the relationship between the seasonal NYS TCs and large-scale climate variability is necessary to improve prediction capability. [Figure 2](#) shows the spatial distribution of correlation coefficients between the observed number of NYS TCs ([Fig. 1b](#)) and

the observed SSTA average for April–May (AM; [Fig. 2a](#)) and July–October (JASO; [Fig. 2b](#)). Using a field significance test ([Wilks 2006](#)), which is conservative concerning spatial correlations, we estimate the false discovery rate (FDR) of erroneously rejected null hypotheses (no correlation) with a test level of 10%. Significant correlations are seen from the tropical central to the eastern Pacific Ocean during both seasons. This finding indicates that the cold phase of ENSO in spring (AM) as well as summer (JASO) could induce higher frequencies of the TCs that affect NYS in the summer compared to climatology. In particular, the strong lag relationship with SST in April–May indicates a potential for NYS TC prediction ahead of the active hurricane season, which is in July–October. Those highly correlated areas in AM SSTA will be selected as potential predictors for NYS TC prediction ([section 4](#)). It has to be noted that these correlations between NYS TCs and SST from the central to eastern Pacific remain significantly high after about 1980 (see discussion in [section 5](#)).

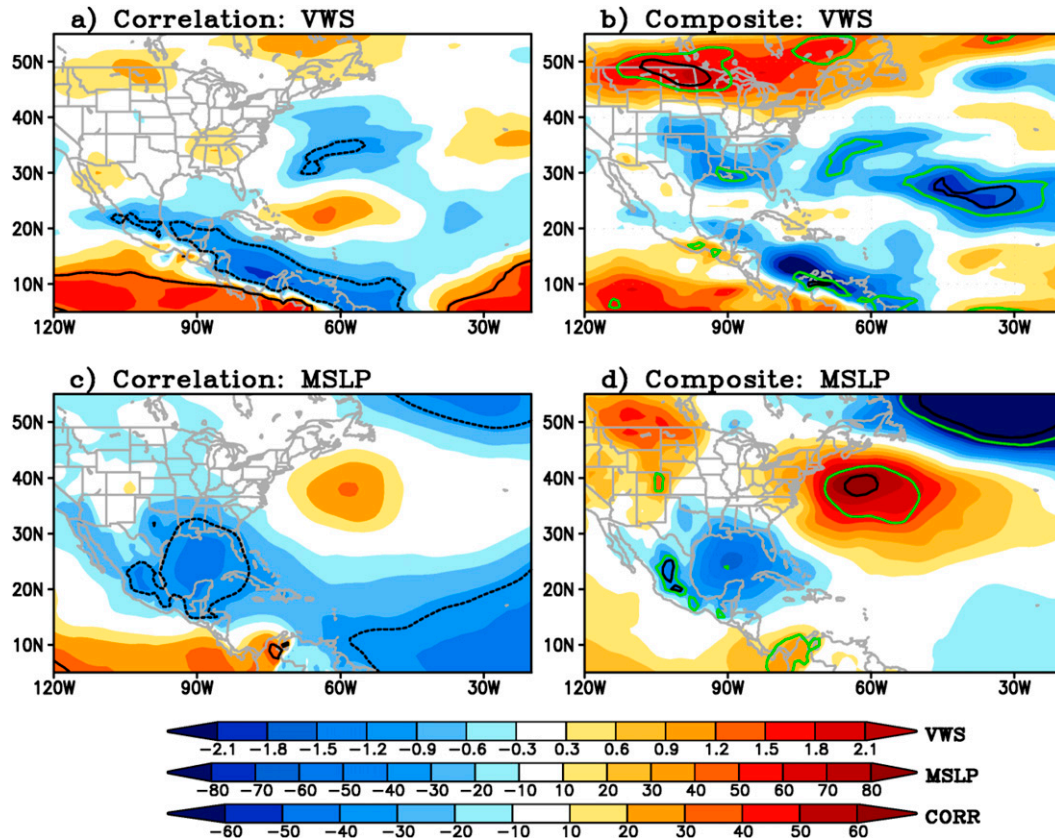


FIG. 3. (left) The spatial distribution of correlation coefficients ($\times 100$) between the number of NYS TCs and the (a) VWS (m s^{-1}) and (c) MSLP (Pa) anomaly over the JASO season. The solid and dashed black lines denote the positive and negative threshold values for the 90% confidence level based on the FDR test, respectively. (right) Composite map of JASO mean (b) VWS (m s^{-1}) and (d) MSLP (hPa) anomaly, over the years when there were one or more NYS TCs. Green (black) contours show statistical significance at the 90% (95%) level computed from bootstrap resampling procedure.

To understand the physical processes of large-scale climate variability on the frequency of NYS TCs, we perform correlation and composite analyses for the atmospheric circulation fields. Figure 3 shows correlations between the number of NYS TCs and the VWS magnitude (Fig. 3a) and MSLP (Fig. 3c) anomaly for the JASO season. Composite maps are the average of JASO VWS (Fig. 3b) and MSLP (Fig. 3d) anomalies of the years when the number of NYS TCs is greater than one (three years: 1979, 1985, and 1999). A bootstrap technique is applied to determine the statistical significance for the composite analysis. A composite anomaly is constructed with 3 years chosen at random from among the 35 years (1979–2013) and this process is repeated 10000 times to obtain a probability distribution at the 90% and 95% levels.

The VWS anomaly driven by ENSO has been known as a major factor that controls the basinwide TC activity (e.g., Gray 1984). A significant decrease in the wind shear magnitude is found over the main TC development region and over most of the North Atlantic basin (Figs. 3a,b).

This anomalous weak wind shear is associated with an anomalous Walker circulation, resulting in changes in the upper-level flow, thus providing favorable conditions for the formation and development of TCs during La Niña events. The large-scale steering flow is the primary contributor to the TC tracks. A significant positive MSLP anomaly in the mid-Atlantic provides favorable conditions for more recurving TCs into NYS (Figs. 3c,d). The anomalous steering flow is characterized by southeasterly wind over the U.S. East Coast, resulting in more TCs passing through NYS during La Niña events. The anomalous circulation at 850 and 500 hPa further supports our argument (Fig. 4).

4. Statistical and statistical–dynamical prediction for seasonal NYS TCs

Based on the physical relationship between the observed NYS TCs and the large-scale variables, a pure statistical model and a statistical–dynamical hybrid model are

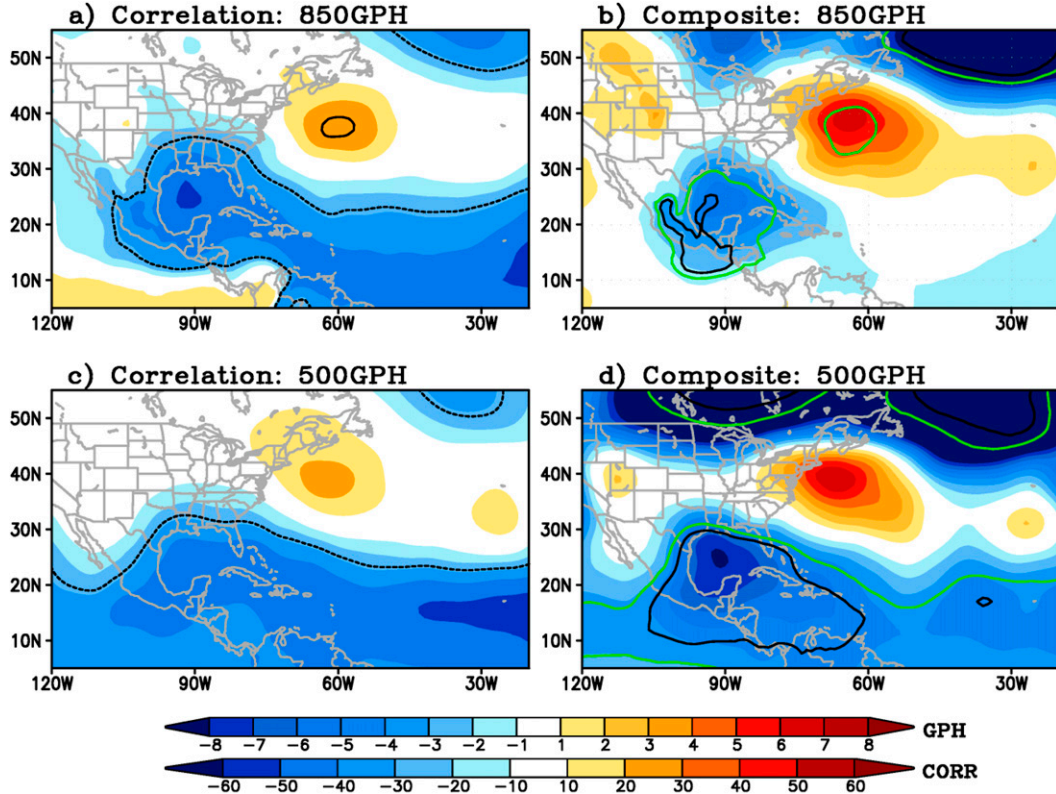


FIG. 4. As in Fig. 3, but for 850- and 500-hPa GPH (m) anomalies.

developed for seasonal prediction of NYS TC numbers. Seasonal prediction for 2014 will be provided as well.

a. Stepwise pattern projection method

For seasonal NYS TC prediction, the stepwise pattern projection method (SPPM) is applied in this study. The SPPM is basically a stepwise regression model that has been applied to seasonal and decadal predictions as well as dynamical model bias correction (Kug et al. 2008; Kim et al. 2014). It produces a prediction of the predictand (e.g., anomalous number of NYS TCs) by projecting the spatial pattern of the predictor field (e.g., SSTA) onto the covariance pattern between the predictor and predictand produced in the training period. The advantage of this model is in the use of flexible geographical predictor domain while all previous hybrid models are restricted to the fixed domain of predictors (Wang et al. 2009; Kim and Webster 2010; Kim et al. 2013; Li et al. 2013). The procedure is as follows. Suppose that the predictand $TC(t)$ is the anomalous number of NYS TCs and the predictor $SST(x, t)$ is the observed SSTA averaged over AM. The spatial and temporal grid points are x and t , respectively. First, over the training period K , the covariance pattern $COV(x)$ between the predictand $TC(t)$ and predictor field $SST(x, t)$ in a certain domain D is computed as

$$COV(x) = \frac{1}{K} \sum_t TC(t) SST(x, t). \quad (1)$$

Then, the predictor field is projected onto the covariance pattern to obtain a single time series $P(t)$:

$$P(t) = \sum_x COV(x) SST(x, t). \quad (2)$$

The regression coefficient α is obtained by the time series $P(t)$ and the predictand $TC(t)$ over the training period K :

$$\alpha = \frac{\sum_t TC(t) P(t)}{\sum_t P(t)^2}. \quad (3)$$

To produce a forecast, the predicted value of $P(t_f)$ can be obtained by projecting the predictor field $SST(x, t_f)$ in the forecast period onto the covariance pattern $COV(x)$, which has already been obtained from the training period:

$$P(t_f) = \sum_x COV(x) SST(x, t_f). \quad (4)$$

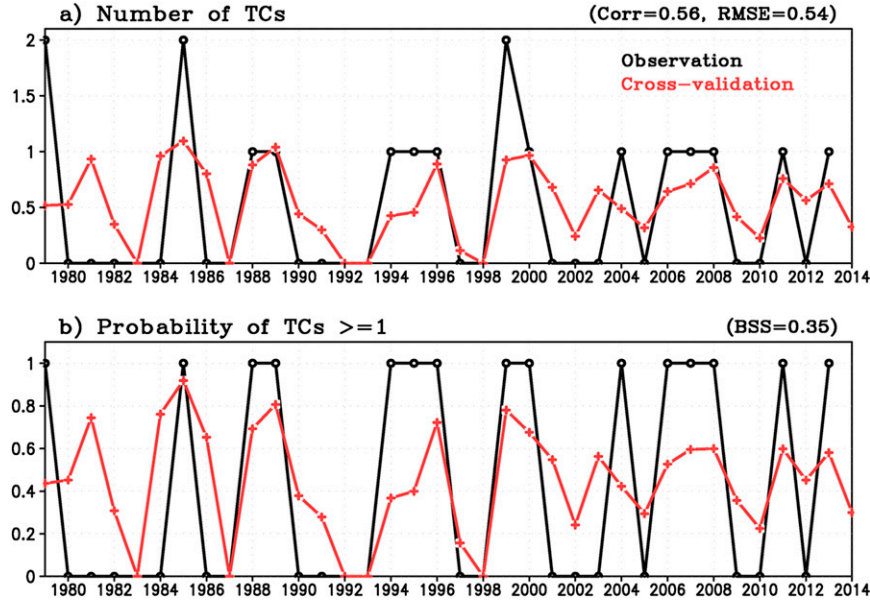


FIG. 5. (a) Number of TCs and (b) probability of the passage of one or more TCs over NYS in the observations (black) and statistical model for June forecast (AM SST as a predictor; red). Correlation coefficients and RMSE between the observed and predicted values and BSS compared to climatology are listed in parentheses.

Finally, by multiplying $P(t_f)$ by the regression coefficient α , the forecasted anomalous number of NYS TCs $TC(t_f)$ can be obtained as

$$TC(t_f) = \alpha P(t_f). \quad (5)$$

Finally, the average number of NYS TCs over the training period is added to the anomaly. It has to be emphasized that the training period and validation period are distinct and a cross-validation method (leave one year out) is applied.

Over the training period, the correlation coefficients between the $TC(t)$ and $SST(x, t)$ are calculated to search for the optimal predictor domain D among all possible grid points within a certain area (10°S – 20°N , 60°W – 180°). The highly correlated grid points (Fig. 2a) are selected as predictors while the grid points slightly change each year in the cross-validation process. The absolute correlation values are used as the criterion for grouping, ranging from 1 to 0.1 in 0.1 intervals. Initially, the grid points that exceed 0.9 are selected. If the number of grid points is less than 300, the grid points with absolute correlation values larger than 0.8 are added, and so on. The limit on the number of grid points (here, 300) is arbitrary, but the results are not sensitive to the choice of the minimum number of grid points or correlation criterion.

b. Statistical prediction for seasonal NYS TCs

Figure 5 shows the observed and predicted numbers of NYS TCs. Although it predicts a lower values than the

observed during the most active years (1979, 1985, and 1999), the model generally performs well, especially during the strong ENSO events (1983, 1987, 1988, 1989, 1992, 1997, 1998, 2000, 2008, 2010, and 2011; Fig. 5a). Cross validation shows that the correlation between the predicted and observed numbers of NYS TCs is as high as 0.56 and the root-mean-square error (RMSE) is 0.54 over the 35 yr for the June forecasts (as it uses AM SST) (Table 2).

Although the SPPM utilized the cross-validated approach, there is still the possibility of overfitting (DelSole and Shukla 2009). Thus, we performed SPPM forecast by separating the time series into two independent periods (1979–96 and 1997–2013). For each period, we use the statistical model trained on data from the other period to predict the number of NYS TCs for that period to confirm whether the cross-validation results are useful. The results (not shown) are very similar to those revealed in Fig. 5a, with the correlation between the predicted and observed numbers being 0.58 when averaged over these two periods. We believe that strong physical linkages between the predictor and predictand result in significant correlations over the entire period; thus, the results from separating the time series into two different periods give almost the same prediction skill as the leave-one-out cross-validation approach. Therefore, we will stay with the cross-validation approach, which has been used in many previous studies for seasonal tropical cyclone prediction (Wang et al. 2009; Kim and

TABLE 2. Correlation coefficients for the numbers of NYS TCs and BSS for the probability of one or more NYS TCs forecast by the statistical (stat) and statistical–dynamical (stat–dyn) models over the period of 1982–2009. For stat–dyn predictions, correlation coefficients and BSS are calculated based on the mean of 24 ensemble members. Boldface indicates values exceeding the 99% confidence level calculated using a 10 000 bootstrap resampling procedure. Numbers listed in parentheses indicate skill over the 35-yr period (1979–2013). Asterisks indicate the model having the higher prediction skill compared to the other.

	Forecast month				
	June	May	April	March	February
Correlation coef (No. of TCs)					
Stat (1979–2013)	0.65* (0.56)	0.56 (0.50)	0.46 (0.42)	0.40 (0.39)	0.36 (0.28)
Stat–dyn	—	0.57*	0.51*	0.57*	0.60*
BSS (TC ≥ 1)					
Stat (1979–2013)	0.44* (0.35)	0.34 (0.30)	0.25 (0.23)	0.20 (0.20)	0.15 (0.14)
Stat–dyn	—	0.35*	0.30*	0.35*	0.34*

Webster 2010; Kim et al. 2013; Li et al. 2013; Klotzbach 2014).

In addition to forecasting the number of NYS TCs, we also attempt to forecast the probability of one or more TCs passing over NYS using the same predictor field (AM SST) with cross validation. Prediction results show high prediction skill with a correlation coefficient of 0.57, which is statistically significant at the 99% level (Fig. 5b). The skill of the probabilistic forecasts can be measured using the Brier skill score (BSS), which in this study uses climatology as the reference forecast. The forecasts of the probability of one or more NYS TCs have a BSS of 0.35 compared to climatology, which is shown to be statistically significant within the 1% confidence level using a 10 000 times bootstrap resampling procedure. The prediction is about 74% correct (26 out of the 35 seasons). Here, correct means no TC passage when the forecast probability was below 50% and vice versa. As a comparison, climatology is correct in 20 out of the 35 seasons in this sense.

The reliability diagram for the probability of one or more NYS TCs is shown in Fig. 6. The forecast probability and observed relative frequency of occurrence is shown. The plot inset shows the percentage of forecasts having probabilities in each of the probability bins (10% interval). The perfect prediction, shown by the diagonal line, occurs when the predicted probability matches the observed frequency, whereas values along a horizontal line indicate a no-skill forecast. In Fig. 6, the predicted probability increases with increasing observed frequency. However, predictions are underconfident, as at very low (high) predicted probabilities, observed probabilities are even lower (higher). It should be noted that the small sample size of predictions and observations (here, only 35) limits our estimation of reliability.

For the 2014 season, the statistical model predicts below average NYS TC activity. The predicted number of TCs passing through NYS in 2014 is 0.33 (climatology 0.51), and the probability of one or more tropical

cyclones (in any stage of their life cycle) crossing New York State is 30%, which is below the climatological probability of 43%. These below average predictions are in agreement with the actual activity (0 NYS TCs).

Since the model described above uses AM observed SSTAs as a predictor, a forecast can be made in early June. This provides useful lead time since most NYS TCs occurred in August and September. To explore the possibility of the extension of the lead time ahead of the active hurricane season, we applied SPPM and used the SST from earlier months. Table 2 shows the prediction skill (correlation and BSS) of predicted numbers

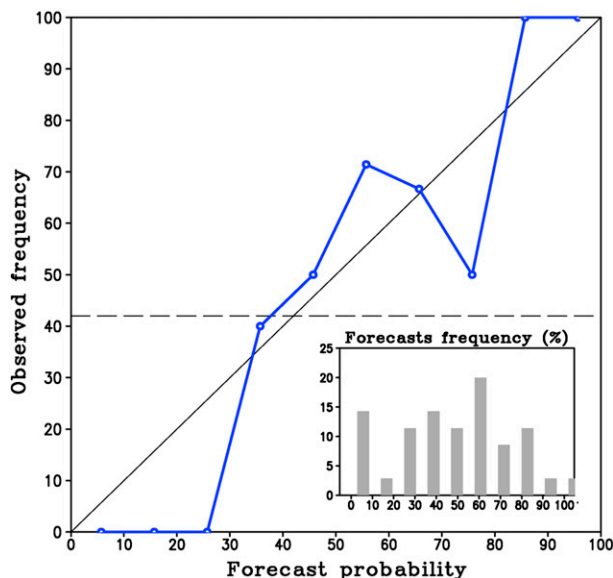


FIG. 6. Reliability diagram of the probability of one or more TC passages over the NYS using a statistical model for the June forecast. The y axis is the relative observed frequency (observed probability) and the x axis is the forecast probability. The diagonal line shows perfect reliability and the horizontal dashed line gives the observed climatological frequency. The inset histogram shows the frequency distribution for predictions among the probability bins.

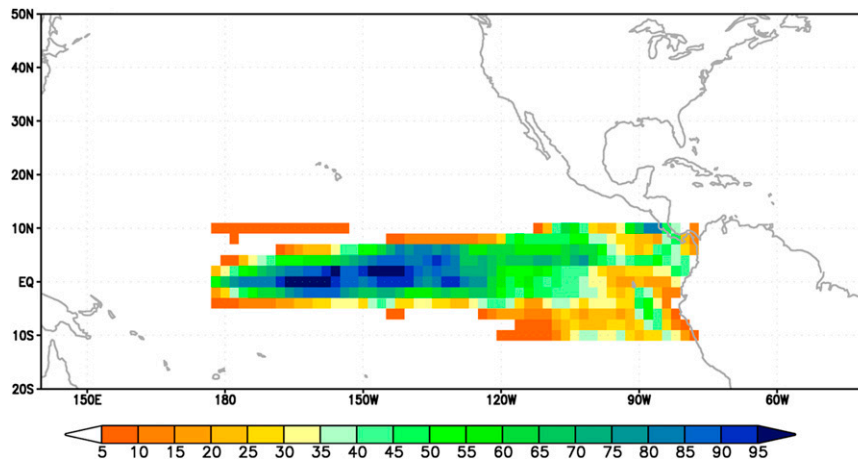


FIG. 7. The selection frequency (%) of CFSv2 SST grid points as a predictor during the SPPM process for the February forecast. The 24 ensemble member's AM SSTA for the February forecast is used as the predictor field.

of NYS TCs and the probability of one or more TCs by forecast issue month. For predictions made in June, we use AM SST as a predictor. For predictions made in May, we use March–April SSTs as a predictor, and so on. The prediction skill decreases as the forecast month gets further ahead of the storm season (Table 2).

c. Statistical–dynamical hybrid forecast

Another way of exploring the possibility of extended prediction is to perform the statistical–dynamical hybrid prediction using predicted fields from dynamical forecasts. This statistically postprocessed dynamical forecast is an instance of the well-known model output statistics (MOS) approach. Benefiting from the significant improvements in dynamical modeling, CFSv2 is able to produce skillful forecasts of tropical Pacific SSTAs (Saha et al. 2014). Instead of using the observed AM SST as a predictor, the SPPM is applied to the predicted AM SST anomaly issued from February to May forecast months. For example, for the February forecast, the predicted AM SSTA made by initial conditions from January to early February is used as the predictor field. For the March forecast, the predicted AM SSTA made by initial conditions from February to early March is used as the predictor field. For the May forecast, the predicted May SSTA from April to early May initial conditions is used as a predictor. It has to be noted that for forecasts made earlier than February, the prediction skill is not significant due to the model capability for ENSO prediction (Xue et al. 2013). The SPPM is applied to individual ensemble members (total of 24 for each forecast month).

As explained in the previous section, over the training period, the highly correlated grid points are selected as

predictors. The distribution of chosen grid points changes slightly depending on the training period. Figure 7 shows the selection frequency (%) of CFSv2 SST grid points as a predictor during the SPPM process for February forecasts. The 24 ensemble member's AM SSTA for the February forecast is used as the predictor field. In Fig. 7, 50% means that a certain grid point is selected 336 times as a predictor over the 28 years among the 24 ensemble members. In most cases, the predictor grids are located over the tropical central Pacific Ocean, but not over the equatorial eastern Pacific Ocean. The slight spatial differences of highly correlated areas from the observation (Fig. 2a) are hypothesized to be due to the CFSv2 model bias that results in lower SSTA prediction skill in the equatorial eastern Pacific Ocean (Kim et al. 2012a,b; Xue et al. 2013).

The prediction skill of NYS TCs by the hybrid model using the 24-member ensemble CFSv2 SST hindcasts issued from February to May are compared in Table 2. The prediction exhibits significant correlation coefficients over all lead times. For the deterministic verifications, only the ensemble mean of the model predictions is used and is treated as a single best-guess forecast. The correlation between predicted (ensemble mean) and observed numbers of NYS TCs is as high as 0.60 and the RMSE is 0.49 over the 28 years for the February forecasts (Fig. 8a). The skill of the hybrid prediction made in February (correlation = 0.60) is just slightly less than the pure statistical prediction made in June (correlation = 0.65) for the same forecast period (1982–2009; Table 2). The forecast of the probability of one or more TCs passing over NYS has a BSS of 0.34 compared to climatology (Fig. 8b). The reliability diagram for the probability of one or more NYS TCs predicted by the 24 ensemble

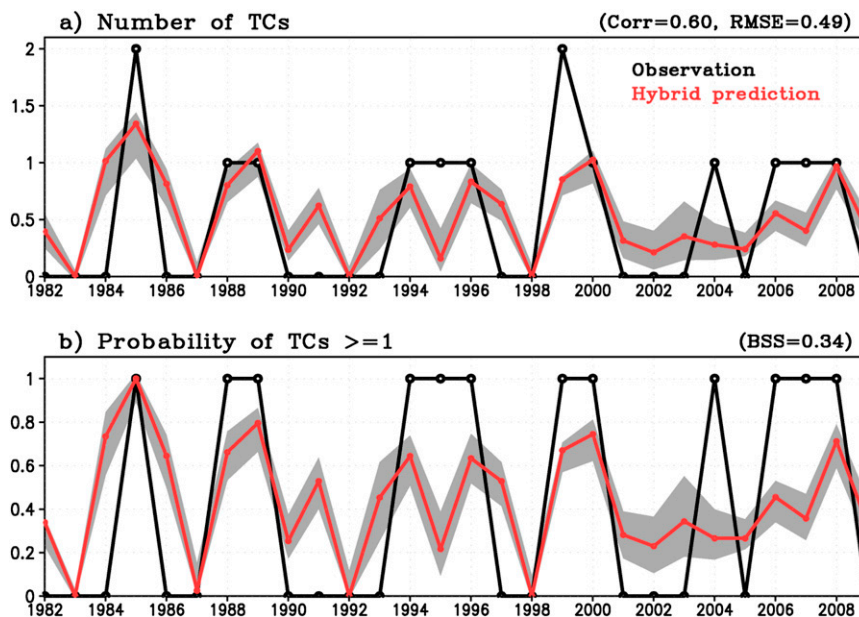


FIG. 8. As in Fig. 5, but for the hybrid prediction using CFSv2 AM SST hindcasts from the February forecast. The red line indicates the results from the ensemble mean and gray shading represents the ranges of one std dev of the 24 ensemble members.

members made in February is shown in Fig. 9. Forecasts are reliable since their reliability curve is close to the diagonal.

For forecasts issued from February to May, both the correlation and the BSS remain significantly high (Table 2). However, it is noticed that the skill of the February forecast is slightly higher compared to those of March and April. We hypothesize that this could be a result of statistical uncertainties due to noise affecting the correlation found in relatively small samples. A rough estimate can be made for the confidence interval for a correlation coefficient of 0.60 (the correlation between the February statistical–dynamical forecast and the observations) using a test proposed by Fisher (see Lindgren 1968), which is appropriate for a large sample size (say $n > 50$). Using this test, the 90% (95%) confidence interval for a correlation coefficient of 0.60 with 28 pairs of data is estimated to be 0.34–0.78 (0.29–0.80). While, strictly speaking, this test is not appropriate for such a small n , it clearly indicates that the difference between correlation coefficients of 0.60 and 0.51 (correlation for the April forecast) is not likely to be statistically significant at any reasonable confidence limit.

Our results indicate that the initial seasonal prediction for NYS TCs can be issued at the beginning of February and updates can be provided from March to May using the hybrid model, with a subsequent update made in June using the pure statistical prediction model.

5. Summary and discussion

A pure statistical prediction model and a statistical–dynamical hybrid prediction model have been developed to forecast NYS TCs based on the physical understanding of the relationship between NYS TCs and the large-scale ocean–atmosphere variability. The circulation anomaly

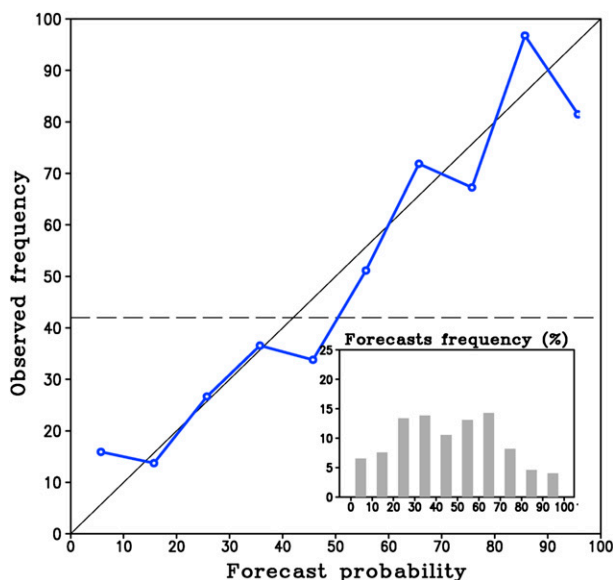


FIG. 9. As in Fig. 6, but for the statistical–dynamical forecast by the 24 ensemble members of CFSv2 AM SST hindcasts from the February forecast.

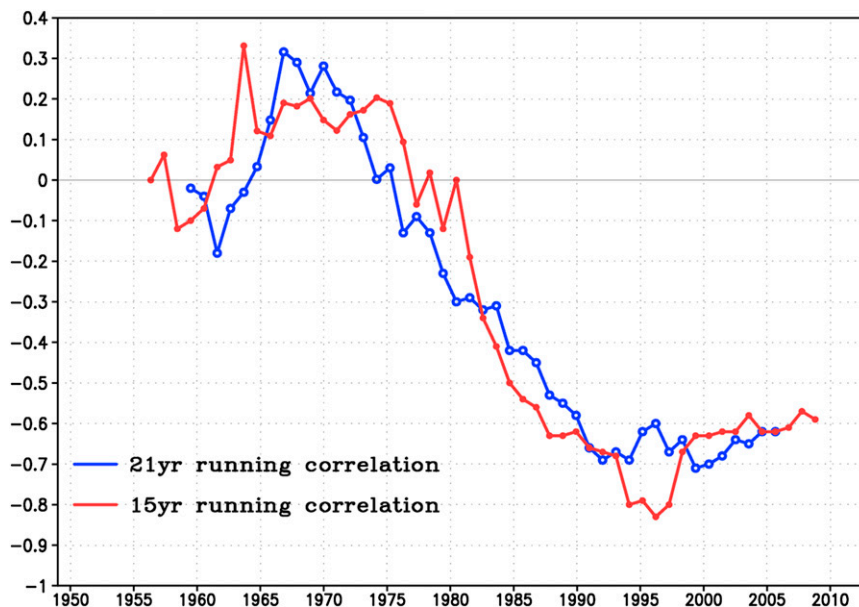


FIG. 10. The 15- (red) and 21-yr (blue) running correlations between the probability of one or more NYS TCs and SSTA over the eastern equatorial Pacific (5°S – 5°N , 180° – 90°W). The year shown corresponds to the center of the period.

in the mid-Atlantic during the cold phase of ENSO provides favorable conditions for more recurring TCs into NYS. Observations and CFSv2 hindcasts are used to statistically downscale the tropical Pacific SST anomaly to forecast the number of NYS TCs and the probability of one or more TCs passing over NYS. For the pure statistical model, cross validation shows that the correlation between observed and predicted seasonal numbers of NYS TCs is as high as 0.56 for the period 1979–2013 for the June forecasts, and forecasts of the probability of one or more tropical cyclones impacting New York State have a BSS of 0.35 compared to climatology. For the 2014 season, the statistical model predicts below average NYS TC activity. The predicted number is 0.33 (climatology 0.51) and the probability of one or more TCs crossing NYS is 30% (climatology 43%). The results of the statistical–dynamical hybrid prediction model show that the current model can provide a skillful preseason prediction in February and updates can be provided in the following months until May.

In this study, we have found a strong relationship between equatorial SSTA and NYS TCs for the period 1979–2013. We have also examined TC and SST data between 1949 and 1978 to see whether this relationship can be found during this earlier period. The 15- and 21-yr running correlations between the probability of one or more TCs affecting New York State and SSTA averaged over the area 5°S – 5°N , 180° – 90°W are shown in Fig. 10. It is clear that during the period after about 1979

(corresponding to after 1989 for the 21-yr running correlation, and 1986 for the 15-yr running correlation), the correlations are consistently large and negative (-0.6 or less) and are highly statistically significant, consistent with our results above that models developed during the early (later) half of this period provide skillful predictions for the later (early) part of the period. However, it is clear from Fig. 10 that this relationship appears to be much weaker or even nonexistent prior to 1979.

One possibility as to why this is the case is that the relationship between SSTA and NYS TCs might be non-stationary. As an example, Klotzbach (2011) has shown that the relationship between U.S. landfalling hurricanes and ENSO is modulated by the phase of the Atlantic multidecadal oscillation. Another possible contributing factor might be larger uncertainties in the number of NYS TCs prior to 1979 as a result of the lack of satellite data for identification and classification of the storms. We believe that the number of NYS TCs is much more uncertain than the number of landfalling hurricanes, since NYS TCs include TCs at all stages of their life cycle including those that have already undergone extratropical transition. In addition, prior to the satellite era, tropical SSTs may also be more uncertain. The running correlations shown in Fig. 10 do not suggest any weakening of this correlation in recent years; hence, we believe that this relationship is still useful, and results presented in Fig. 3 also suggest that the relationship is physically sound. Meanwhile, careful monitoring of this relationship, as well as further

research into clarifying what might have given rise to changes in the relationship before 1979, should be conducted. Nevertheless, it should be emphasized that the correlation found between equatorial Pacific SSTA and the probability of one of more TCs affecting New York State during the 35-yr period of 1979–2013 (-0.60) is statistically significant at the 99.98% level and is unlikely to be due to chance alone.

Although the statistical–dynamical prediction model provides significant skill for NYS TCs, the model can be improved in several ways. First, the current prediction model is limited to the use of the SST anomaly as a single predictor. Additional skill may arise by considering other relevant thermodynamic and dynamic variables, as well as the time evolution of the slowly varying climate signals as predictors. Second, the analysis and prediction of TC properties is limited to the number of NYS TCs. Accumulated Cyclone Energy could be a more suitable parameter for examining the TC activity as it combines the number, lifetime, and intensity of TCs. Third, it is known that different models possess their own systematic character, and seasonal prediction skill also improves with model diversity apart from improvements from larger ensemble size (DelSole et al. 2014). Therefore, by using a large set of ensemble members from multimodel dynamical forecast systems, useful information concerning probabilistic forecasts can be provided to end users, especially those who live in the vicinity of New York State. For future work, we plan to develop an advanced hybrid model with various physically relevant predictors using the North American Multimodel Ensemble (NMME; Kirtman et al. 2014) hindcasts–forecasts and assess the possibility for real-time probabilistic forecasts for NYS TC activity using a multimodel ensemble approach.

In this study, we have demonstrated that skillful models can be developed for the seasonal prediction of NYS TCs. It is worth reemphasizing that our predictand is the number of TCs that cross NYS during their lifetimes, including TCs that are no longer categorized as hurricanes when they reach NYS. We hypothesize that our models work well partly because the TCs crossing NYS all took relatively similar paths (Fig. 1a). Our results suggest that similar strategies could also work in other regions over which TC tracks are more or less homogeneous, and useful prediction models for other locations (such as New England) may also be developed based on the methodology employed in this study.

Acknowledgments. The constructive and valuable comments of the four anonymous reviewers are greatly appreciated. The authors would also like to thank Albert Yau for assistance in preparing some of the data

used in this study. This work was supported by NYS RISE. HMK was also supported by the Korea Meteorological Administration Research and Development Program under Grant APCC 2013-3141.

REFERENCES

- Avila, L. A., and J. Cangialos, 2011: Hurricane Irene. Tropical Cyclone Rep. AL092011, National Hurricane Center, 45 pp. [Available online at http://www.nhc.noaa.gov/data/tcr/AL092011_Irene.pdf.]
- Barnston, A. G., and M. K. Tippett, 2013: Predictions of Nino3.4 SST in CFSv1 and CFSv2: A diagnostic comparison. *Climate Dyn.*, **41**, 1615–1633, doi:10.1007/s00382-013-1845-2.
- Bell, G. D., and Coauthors, 2000: Climate assessment for 1999. *Bull. Amer. Meteor. Soc.*, **81** (6), S1–S50, doi:10.1175/1520-0477(2000)81[s1:CAF]2.0.CO;2.
- Berrisford, P., D. Dee, K. Fielding, M. Fuentes, P. Kallberg, S. Kobayashi, and S. Uppala, 2009: The ERA-Interim archive. ERA Rep. Series, No. 1, ECMWF, Reading, United Kingdom, 16 pp.
- Bove, M. C., J. J. O'Brien, J. B. Elsner, C. W. Landsea, and X. Niu, 1998: Effect of El Niño on U.S. landfalling hurricanes, revisited. *Bull. Amer. Meteor. Soc.*, **79**, 2477–2482, doi:10.1175/1520-0477(1998)079<2477:EOENOO>2.0.CO;2.
- Camargo, S. J., A. G. Barnston, P. J. Klotzbach, and C. W. Landsea, 2007a: Seasonal tropical cyclone forecasts. *WMO Bull.*, **56**, 297–309.
- , A. W. Robertson, S. J. Gaffney, P. Smyth, and M. Ghil, 2007b: Cluster analysis of typhoon tracks: Part II: Large-scale circulation and ENSO. *J. Climate*, **20**, 3654–3676, doi:10.1175/JCLI4203.1.
- Colbert, A. J., and B. J. Soden, 2012: Climatological variations in North Atlantic tropical cyclone tracks. *J. Climate*, **25**, 657–673, doi:10.1175/JCLI-D-11-00034.1.
- DelSole, T., and J. Shukla, 2009: Artificial skill due to predictor screening. *J. Climate*, **22**, 331–345, doi:10.1175/2008JCLI2414.1.
- , J. Nattala, and M. K. Tippett, 2014: Skill improvement from increased ensemble size and model diversity. *Geophys. Res. Lett.*, **41**, 7331–7342, doi:10.1002/2014GL060133.
- Elsner, J. B., 2003: Tracking hurricanes. *Bull. Amer. Meteor. Soc.*, **84**, 353–356, doi:10.1175/BAMS-84-3-353.
- Goldenberg, S. B., and L. J. Shapiro, 1996: Physical mechanisms for the association of El Niño and West African rainfall with Atlantic major hurricane activity. *J. Climate*, **9**, 1169–1187, doi:10.1175/1520-0442(1996)009<1169:PMFTAO>2.0.CO;2.
- Gray, W. M., 1984: Atlantic seasonal hurricane frequency. Part I: El Niño and 30 mb quasi-biennial oscillation influences. *Mon. Wea. Rev.*, **112**, 1649–1668, doi:10.1175/1520-0493(1984)112<1649:ASHFPI>2.0.CO;2.
- Higgins, R. W., J. E. Janowiak, and Y. P. Yao, 1996: A gridded hourly precipitation data base for the United States (1963–1993). NCEP/Climate Prediction Center Atlas 1, 47 pp.
- Kim, H. M., and P. J. Webster, 2010: Extended-range seasonal hurricane forecasts for the North Atlantic with hybrid dynamical–statistical model. *Geophys. Res. Lett.*, **37**, L21705, doi:10.1029/2010GL044792.
- , —, and J. A. Curry, 2012a: Seasonal prediction skill of ECMWF System 4 and NCEP CFSv2 retrospective forecast for the Northern Hemisphere winter. *Climate Dyn.*, **12**, 2957–2973, doi:10.1007/s00382-012-1364-6.
- , —, —, and V. Toma, 2012b: Asian summer monsoon prediction in ECMWF System 4 and NCEP CFSv2 retrospective

- seasonal forecasts. *Climate Dyn.*, **39**, 2975–2991, doi:[10.1007/s00382-012-1470-5](https://doi.org/10.1007/s00382-012-1470-5).
- , M. I. Lee, P. J. Webster, D. Kim, and J. H. Yoo, 2013: A physical basis for the probabilistic prediction of the accumulated tropical cyclone kinetic energy in the western North Pacific. *J. Climate*, **26**, 7981–7991, doi:[10.1175/JCLI-D-12-00679.1](https://doi.org/10.1175/JCLI-D-12-00679.1).
- , Y. G. Ham, and A. A. Scaife, 2014: Improvement of initialized decadal predictions over the North Pacific Ocean by systematic anomaly pattern correction. *J. Climate*, **27**, 5148–5162, doi:[10.1175/JCLI-D-13-00519.1](https://doi.org/10.1175/JCLI-D-13-00519.1).
- Kirtman, B. P., and Coauthors, 2014: The North American Multi-model Ensemble: Phase-1 seasonal-to-interannual prediction; phase-2 toward developing intraseasonal prediction. *Bull. Amer. Meteor. Soc.*, **95**, 585–601, doi:[10.1175/BAMS-D-12-00050.1](https://doi.org/10.1175/BAMS-D-12-00050.1).
- Klotzbach, P. J., 2011: El Niño–Southern Oscillation’s impact on Atlantic basin hurricanes and U.S. landfalls. *J. Climate*, **24**, 1252–1263, doi:[10.1175/2010JCLI3799.1](https://doi.org/10.1175/2010JCLI3799.1).
- , 2014: Prediction of seasonal Atlantic basin accumulated cyclone energy from 1 July. *Wea. Forecasting*, **29**, 115–121, doi:[10.1175/WAF-D-13-00073.1](https://doi.org/10.1175/WAF-D-13-00073.1).
- Kossin, J. P., D. J. Vimont, and M. Sitkowski, 2010: Climate modulation of North Atlantic hurricane tracks. *J. Climate*, **23**, 3057–3076, doi:[10.1175/2010JCLI3497.1](https://doi.org/10.1175/2010JCLI3497.1).
- Kug, J. S., J. Y. Lee, and I. S. Kang, 2008: Systematic error correction of dynamical seasonal prediction using a stepwise pattern projection method. *Mon. Wea. Rev.*, **136**, 3501–3512, doi:[10.1175/2008MWR2272.1](https://doi.org/10.1175/2008MWR2272.1).
- Landsea, C. W., J. L. Franklin, 2013: Atlantic Hurricane Database uncertainty and presentation of a new database format. *Mon. Wea. Rev.*, **141**, 3576–3592, doi:[10.1175/MWR-D-12-00254.1](https://doi.org/10.1175/MWR-D-12-00254.1).
- Li, X., S. Yang, H. Wang, X. Jia, and A. Kumar, 2013: A dynamical–statistical forecast model for the annual frequency of western Pacific tropical cyclones based on the NCEP Climate Forecast System version 2. *J. Geophys. Res.*, **118**, 12 061–12 074, doi:[10.1002/2013JD020708](https://doi.org/10.1002/2013JD020708).
- Lindgren, B. W., 1968: *Statistical Theory*. 3rd ed. Macmillan, 614 pp.
- Mesinger, F., and Coauthors, 2006: North American Regional Reanalysis. *Bull. Amer. Meteor. Soc.*, **87**, 343–360, doi:[10.1175/BAMS-87-3-343](https://doi.org/10.1175/BAMS-87-3-343).
- Saha, S., and Coauthors, 2010: The NCEP Climate Forecast System Reanalysis. *Bull. Amer. Meteor. Soc.*, **91**, 1015–1057, doi:[10.1175/2010BAMS3001.1](https://doi.org/10.1175/2010BAMS3001.1).
- , and Coauthors, 2014: The NCEP Climate Forecast System version 2. *J. Climate*, **27**, 2185–2208, doi:[10.1175/JCLI-D-12-00823.1](https://doi.org/10.1175/JCLI-D-12-00823.1).
- Smith, S. R., J. Brolley, J. J. O’Brien, and C. A. Tartaglione, 2007: ENSO’s impact on regional U.S. hurricane activity. *J. Climate*, **20**, 1404–1414, doi:[10.1175/JCLI4063.1](https://doi.org/10.1175/JCLI4063.1).
- Smith, T. M., R. W. Reynolds, T. C. Peterson, and J. Lawrimore, 2008: Improvements to NOAA’s historical merged land–ocean temperature analysis (1880–2006). *J. Climate*, **21**, 2283–2296, doi:[10.1175/2007JCLI2100.1](https://doi.org/10.1175/2007JCLI2100.1).
- Tang, B. H., and J. D. Neelin, 2004: ENSO influence on Atlantic hurricanes via tropospheric warming. *Geophys. Res. Lett.*, **31**, L24204, doi:[10.1029/2004GL021072](https://doi.org/10.1029/2004GL021072).
- Vecchi, G. A., M. Zhao, H. Wang, G. Villarini, A. Rosati, A. Kumar, I. M. Held, and R. Gudgel, 2011: Statistical–dynamical predictions of seasonal North Atlantic hurricane activity. *Mon. Wea. Rev.*, **139**, 1070–1082, doi:[10.1175/2010MWR3499.1](https://doi.org/10.1175/2010MWR3499.1).
- Vimont, D. J., and J. P. Kossin, 2007: The Atlantic meridional mode and hurricane activity. *Geophys. Res. Lett.*, **34**, L07709, doi:[10.1029/2007GL029683](https://doi.org/10.1029/2007GL029683).
- Wang, H., J.-K. E. Schemm, A. Kumar, W. Wang, L. Long, M. Chelliah, G. D. Bell, and P. Peng, 2009: A statistical forecast model for Atlantic seasonal hurricane activity based on the NCEP dynamical seasonal forecast. *J. Climate*, **22**, 4481–4500, doi:[10.1175/2009JCLI2753.1](https://doi.org/10.1175/2009JCLI2753.1).
- Wilks, D. S., 2006: *Statistical Methods in the Atmospheric Sciences*. 2nd ed. International Geophysics Series, Vol. 91, Academic Press, 627 pp.
- Xue, Y., M. Chen, A. Kumar, Z. Z. Hu, and W. Wang, 2013: Prediction skill and bias of tropical Pacific sea surface temperatures in the NCEP Climate Forecast System version 2. *J. Climate*, **26**, 5358–5378, doi:[10.1175/JCLI-D-12-00600.1](https://doi.org/10.1175/JCLI-D-12-00600.1).